Toxicology Mechanisms and Methods

ISSN: (Print) (Online) Journal homepage: www.tandfonline.com/journals/itxm20

Naturally-derived phenethyl isothiocyanate modulates apoptotic induction through regulation of the intrinsic cascade and resulting apoptosome formation in human malignant melanoma cells

Venetia Tragkola, Ioannis Anestopoulos, Sotiris Kyriakou, Tom Amery, Rodrigo Franco, Aglaia Pappa & Mihalis I. Panayiotidis

To cite this article: Venetia Tragkola, Ioannis Anestopoulos, Sotiris Kyriakou, Tom Amery, Rodrigo Franco, Aglaia Pappa & Mihalis I. Panayiotidis (25 Jun 2024): Naturally-derived phenethyl isothiocyanate modulates apoptotic induction through regulation of the intrinsic cascade and resulting apoptosome formation in human malignant melanoma cells, Toxicology Mechanisms and Methods, DOI: 10.1080/15376516.2024.2369666

To link to this article: https://doi.org/10.1080/15376516.2024.2369666

TOXICOLOGY MECHANISMS AND METHODS
https://doi.org/10.1080/15376516.2024.2369666

Taylor & Francis
Taylor & Francis Group

RESEARCH ARTICLE

Naturally-derived phenethyl isothiocyanate modulates apoptotic induction through regulation of the intrinsic cascade and resulting apoptosome formation in human malignant melanoma cells

Venetia Tragkola[a], Ioannis Anestopoulos[a], Sotiris Kyriakou[a], Tom Amery[b], Rodrigo Franco[c], Aglaia Pappa[d] and Mihalis I. Panayiotidis[a]

[a]Department of Cancer Genetics, Therapeutics & Ultrastructural Pathology, The Cyprus Institute of Neurology & Genetics, Nicosia, Cyprus; [b]Watercress Company, Dorchester, UK; [c]School of Veterinary Medicine & Biomedical Sciences, University of Nebraska-Lincoln, Lincoln, NE, USA; [d]Department of Molecular Biology & Genetics, Democritus University of Thrace, Alexandroupolis, Greece

ABSTRACT

Malignant melanoma is the most aggressive type of skin cancer with increasing incidence rates worldwide. On the other hand, watercress is a rich source of phenethyl isothiocyanate (PEITC), among others, which has been widely investigated for its anticancer properties against various cancers. In the present study, we evaluated the role of a watercress extract in modulating apoptotic induction in an *in vitro* model of human malignant melanoma consisting of melanoma (A375, COLO-679, COLO-800), non-melanoma epidermoid carcinoma (A431) and immortalized, non-tumorigenic keratinocyte (HaCaT) cells. Moreover, the chemical composition of the watercress extract was characterized through UPLC MS/MS and other analytical methodologies. In addition, cytotoxicity was assessed by the alamar blue assay whereas apoptosis was determined, initially, by a multiplex activity assay kit (measuring levels of activated caspases −3, −8 and −9) as well as by qRT-PCR for the identification of major genes regulating apoptosis. In addition, protein expression levels were evaluated by western immunoblotting. Our data indicate that the extract contains various phytochemicals (e.g. phenolics, flavonoids, pigments, etc.) while isothiocyanates (ITCs; especially PEITC) were the most abundant. In addition, the extract was shown to exert a significant time- and dose-dependent cytotoxicity against all malignant melanoma cell lines while non-melanoma and non-tumorigenic cells exhibited significant resistance. Finally, expression profiling revealed a number of genes (and corresponding proteins) being implicated in regulating apoptotic induction through activation of the intrinsic apoptotic cascade. Overall, our data indicate the potential of PEITC as a promising anti-cancer agent in the clinical management of human malignant melanoma.

ARTICLE HISTORY
Received 29 April 2024
Revised 12 June 2024
Accepted 13 June 2024

KEYWORDS
Watercress; isothiocyanates; phenethyl isothiocyanate; glucosinolates; malignant melanoma; apoptosis

1. Introduction

Malignant melanoma is the most common and lethal type of skin cancer associated with high rates of incidence and mortality worldwide (Bolick and Geller 2021). Although the development of recent therapeutic approaches (e.g. immunotherapy and targeted therapy) have shown some clinical benefit [Alqathama 2020; Anestopoulos et al. 2022; Esfahani et al. 2020], survival rates among metastatic melanoma patients are still low due to acquired drug-resistance mechanisms (Huang and Zappasodi 2022; Zhong et al. 2022). In this context, the development of novel and alternative therapeutic options is of paramount importance.

Plant-derived compounds have been widely described for their use against various pathological conditions, including cancer, through pleiotropic mechanisms (Chen et al. 2018; Chikara et al. 2018). Specifically, various bioactive phytochemicals have attracted significant scientific interest due to their health-promoting properties. These are categorized as organosulfur, phenolic, nitrogen-containing and carotenoid compounds (Mitsiogianni et al. 2019). Isothiocyanates (ITCs) are secondary bioactive plant metabolites yielded upon the hydrolysis of their precursor (inactive) glucosinolate (GLs) molecules which is catalyzed by an endogenous myrosinase activated upon plant disruption (i.e. cutting, chewing etc.) (Barba et al. 2016; Narbad and Rossiter 2018). Moreover, several environmental factors (e.g. pH, ferrous ions and ascorbic acid concentration) can affect the activation of myrosinase and ultimately the overall bioconversion process of GLs (Shakour et al. 2022). In this way, a plethora of ITCs can be generated dependent on the type of side chain of their respective GL, such as sulforaphane (SFN), iberin (IBN), allyl (AITC), benzyl (BITC) and phenethyl (PEITC) (Sikorska-Zimny and Beneduce 2021; Zhang 2012). To this end, *Nasturtium officinale* (also known as watercress) belongs to the family of *Brassicaceae* and it is described as an exceptional source of

CONTACT Mihalis I. Panayiotidis mihalisp@cing.ac.cy Department of Cancer Genetics, Therapeutics & Ultrastructural Pathology, The Cyprus Institute of Neurology & Genetics, 6 Iroon Avenue, Ayios Dometios, Nicosia, 2371, Cyprus
Supplemental data for this article can be accessed online at https://doi.org/10.1080/15376516.2024.2369666.

PEITC among other phytochemicals (e.g. phenolics, flavonoids, etc.). Several studies report the anticancer potency of watercress extracts in various cancer models (including melanoma) through activation of apoptosis (Rose et al. 2005; Boyd et al. 2006; Pereira et al. 2017; Kyriakou et al. 2022a).

In this study, we aimed to (i) characterize the phytochemical content of lyophilized organic watercress powder as a natural source of PEITC and (ii) delineate its anticancer activity in a human malignant melanoma model consisting of melanoma (A375, COLO-679, COLO-800), non-melanoma epidermoid carcinoma (A431) and non-tumorigenic immortalized keratinocyte (HaCaT) cells.

2. Materials & methods

2.1. Materials and reagents

Hexane ≥97%, methanol HPLC grade ≥99.9%, water HPLC grade, acetonitrile HPLC grade ≥99.9% and acetone ≥ 99.8% were purchased from Honeywell (Charlotte, NC, USA). Folin-Ciocalteau-based polyphenol quantification assay kit was purchased from BioQuoChem (Spain). Sulfuric acid 95–97%, acetic acid ≥99.7%, *tert*-Butyl hydroperoxide (TBH), sodium chloride, tris base and Tween-20 were obtained from Sigma Aldrich (Saint Louis, MO, USA). Trifluoroacetic acid (TFA; LC-MS grade), BCA protein assay kit and SuperSignal™ West Pico PLUS chemiluminescent substrate were purchased from Thermofisher Scientific (Waltham, MA, USA). Dulbecco's Modified Eagle Medium (DMEM) - high glucose culture medium, RPMI 1640 culture medium, phosphate-buffered saline (PBS), *L*-glutamine, Penicillin-Streptomycin, trypsin-EDTA 100× were purchased from Biosera (East Sussex, UK). Fetal bovine serum (FBS) and dimethyl sulfoxide (DMSO) were purchased from PanBiotech (Aidenbach, Germany). Resazurin sodium salt, SDS and sodium deoxycholate were purchased from Fluorochem (Derbyshire, UK) and Trypan Blue from Gibco (Paisley, Scotland). NS3694 apoptosome inhibitor and SYBR Green qPCR Master Mix (High ROX) were purchased from Medchem (Monmouth Junction, NJ, USA). Caspases-3, −8 and −9 multiplex activity assay kit was purchased from Abcam (Cambridge, UK), µ-plate 96 well black plate from Ibidi (Gräfelfing, Germany), NucleoZol reagent from Macherey-Nagel (Germany), PrimeScript™ RT Reagent kit from TaKaRa (France), 96-well semi skirted PCR plates from Azenta (Burlington, MA, USA), microAMP™ optical adhesive film from Applied Biosystems (Foster City, CA, USA), FastGene PAGE gels (gradient: 4–20%, 10 × 8 cm) and MOPs running buffer from Nippon Genetics (Düren, Germany). Polyvinylidene difluoride (PVDF) membranes were purchased from GE Healthcare Life Sciences (Chicago, IL, USA), 95% ethanol denatured, isopropanol and glycine from Carlo Erba (Emmendingen, Germany), water for injections from DEMO S.A. (Krioneri, Greece) and bovine serum albumin from Fisher Chemicals (Hampton, NH, USA). Bromophenol blue was purchased from Honeywell (Medisell, Cyprus) while Pierce protease and phosphatase inhibitor mini tablets kit from Thermo Scientific (Waltham, MA, USA). All primary antibodies used such as anti-Caspase-2 (#2224), anti-caspase-9 (#9508), anti-Bcl-XL, anti-cytochrome c (#11940), anti-Bax (#41162), anti-FLIP (#56343), anti-DCR2 (#8049) and anti-Bcl2 (#4223) were purchased from Cell Signaling Technologies (Boston, MA, USA). Furthermore, anti-GAPDH (6C6) (#sc-32233) and anti-β-actin (MA5) (#15739) were purchased from Santa Cruz Biotechnology (Dallas, TX, USA). All analytical standards were purchased from Extrasynthese (Lyon, France). Finally, 75cm^2 cell culture flasks (#70075), cell culture dishes (#20101) and 96-well cell culture plates (#30096) were purchased from SPL Life Sciences (Pochon, Kyonggi-do, South Korea).

2.2. Extraction of GLs

GLs were extracted according to Kyriakou et al. (2022b). Briefly, one (1.0) gram of watercress powder was mixed with 70% *v/v* (aqueous) methanol and heated at 80^{0}C for 30 min. Then, the resulting solution was sonicated at 37 °C for further 30 min and centrifuged at 3,000 × *g* for 20 min. One (1.0) mL of supernatant was diluted in 9 mL ultrapure water and the solution was filtered through a 0.22 µm (mixed cellulose esters, MCE) filter. UPLC MS/MS was utilized to analyze the final filtered mixture.

2.3. Hydrolysis of GLs, isolation and derivatization of ITCs

Watercress, on its lyophilized form (powder), was kindly provided by The Watercress Company, Dorchester, Dorset, UK and stored at −20 °C in a sealed bag protected from air, light and humidity until further use. The extraction procedure was performed according to Kyriakou et al. (2022a). Briefly, for the extraction of ITCs enriched fractions, five (5.0) grams of watercress powder was stirred vigorously with 315 mL of phosphate-buffered saline (PBS) (pH 7.4) for 1.5 hr (containing a catalytic amount of ascorbic acid to prevent the rearrangement of isothiocyanates) at 37 °C. In order to isolate each of the ITCs, different solvents were used. For the PEITC-enriched extract, 400 mL of hexane solvent was added to the mixture, while for the extraction of IBN, SFN, BITC and indole-3-carbinol, 400 mL of dichloromethane was utilized instead. Finally, AITC extraction was achieved using diethyl ether. All of the hydrolyzed mixtures were stirred, for 2 hr, at room temperature (RT). The organic phase was separated and filtered using a Büchner Funnel with a Whatman paper (pore size: 4.0 – 12.0 µm). The organic phase was dried through magnesium sulfate. The extract was then concentrated to dryness at 40 °C under reduced pressure. The isolated extracts were stored at −20 °C until further use. For the derivatization of ITCs, the extracts were mixed with acetonitrile and filtered through a 0.22 µm MCE (mixed cellulose esters) membrane. PEITC, IBN, SFN, AITC and BITC filtered solutions were immediately mixed with 500 µL of 2 M ammonia/isopropanol and incubated, at RT, for 24 hr. The following day, the excess of solvents was evaporated under reduced pressure and the isolated solid material was reconstituted in (LC-MS grade) methanol: 0.1% *v/v* TFA mixture (4:1). In contrast, Indole-3- carbinol extract was directly reconstituted in methanol: 0.1% *v/v* TFA mixture (4:1).

2.4. Extraction of polyphenols

Polyphenolic compounds were extracted according to Kyriakou et al. (2022a). In brief, one (1.0) gram watercress powder was macerated in 80% *v/v* (aqueous) methanol at 80^0C, for 48 hr, and then filtered in Whatman paper (pore size: 4.0 – 12 µm). This process was repeated twice. The resulting solution was dried and then reconstituted in methanol (LC-MS grade). The final fraction was syringe-filtered through a 0.22 µm MCE filter and analyzed by UPLC-MS/MS.

2.5. Analytical standard and sample preparation

The standard preparation was performed according to Kyriakou et al. (2022b). In brief, stock solutions of the standard compounds were prepared in either methanol or methanol: acetonitrile (1:1) mixture of methanol 70% *v/v* (aqueous) at a final concentration of 1,000 ppm whereas watercress powder extracts were reconstituted in ice-cold methanol until reaching 25 ppb and stored at −20 °C, until further use. Both samples and standards were filtered in a 0.22 µm membrane before analysis was performed by UPLC-QqQ- ESI MS/MS.

2.6. Quantification of ITCs, GLs and polyphenols

2.6.1. Liquid chromatography (LC) conditions

A Waters Acquity UPLC system (Waters Corp., Milford, MA, USA) was employed equipped with two pumps, a degasser and an autosampler. The above compounds were separated in an ACQUITY UPLC BEH C18 (100 × 2.1 mm, particle size: 1.7 µM) column heated at 30 °C by using the elution gradients as previously described by Kyriakou et al. (2022b). The separation of derivatized ITCs, indole-3-carbinol and intact GLs was performed according to Kyriakou et al. (2022b).

2.6.2. Tandem mass spectrometry (MS/MS) conditions

For the MS/MS experimental set-up, a Xevo Triple Quatrapole (TQD) Mass detector (Waters Corp., Milford, MA, USA) was used by utilizing an electron spray ionization in either positive or negative mode (ESI±). Quantitative analysis was performed using a multiple reaction monitoring (MRM) mode. The MRM conditions were optimized specifically for each standard compound by manual tuning of each standard (1 ppm concentration) prior to sample analysis (Tables S1–S3, Supplementary Info). For maximum signal acquisition, the optimized tuning parameters were as follows: capillary voltage: 2.5–3.0 kV; cone voltage: 36 V; source temperature: 150 °C; disolvation temperature: 500 °C; source disolvating gas flow: 1000 L/hr and gas flow: 20 L/hr. High-purity nitrogen gas was used as the drying and nebulizing gas whereas ultrahigh-purity argon was used as a collision gas. Data acquisition and processing were performed on MassLynx software (version 4.1).

2.7. Determination of total flavonoid content (TFC)

The aluminum chloride method was utilized to determine TFC. Briefly, the watercress powder extract was dissolved in acetonitrile. Then, 20 µL of the watercress powder extract were dissolved with 60 µL of methanol and thoroughly mixed with 10 µL of aluminum chloride (10% aqueous solution) and 10 µL of sodium acetate (0.5 M aqueous solution). The resulting solutions were incubated, for 45 min, at 37 °C protected from light. Standard solutions of catechin and rutin were prepared similarly and a standard curve was prepared. The absorbance was measured at 415 nm and the total flavonoid content was estimated based on both catechin (linear range: 0–100 µg/mL; R^2> 0.979) and rutin (linear range: 0–500 µg/mL; R^2> 0.993) calibration curves. Data were expressed as µg of catechin (CE) or µg of rutin (RE) equivalents/g of dry extract.

2.8. Determination of total phenolic content (TPC)

Initially, the watercress powder extract was dissolved in acetonitrile. The Folin-Ciocalteau-based polyphenol quantification assay kit (BioQuoChem, Spain) was used following the manufacturer's instructions for the determination of TPC. The absorbance was measured at 690 nm and TPC was determined based on the gallic acid calibration curve (linear range: 0–400 µg/mL; R^2> 0.995). Data were expressed as µg of gallic acid equivalents (GAE)/g of dry extract.

2.9. Determination of pigments

Chlorophylls -a and -b, lycopene and β-carotene determinations were performed as described by Kyriakou et al. (2022a). Briefly, five (5.0) grams of watercress powder were mixed with 100 mL of acetone/hexane mixture at a 4:6 *v/v* ratio. The solution was vigorously stirred, for 10 hr, and filtered through a Whatman filter paper. The absorbance was measured sequentially at 453, 505, 645, and 663 nm. Pigments were estimated based on the following equations (Equations (1)–(4)):

$$\beta-\text{Carotene}=\left[0.216\times A_{663}-1.22\times A_{645}-0.304\times A_{505}+0.452\times A_{453}\right]/20 \quad (1)$$

$$\text{Lycopene}=\left[-0.0458\times A_{663}+0.204\times A_{645}+0.372\times A_{505}-0.0806\times A_{453}\right]/20 \quad (2)$$

$$\text{Chlorophyll A}=\left[0.999\times A_{663}-0.0989\times A_{645}\right]/20 \quad (3)$$

$$\text{Chlorophyll B}=\left[1.77\times A_{645}-0.328\times A_{663}\right]/20 \quad (4)$$

2.10. Determination of total soluble protein content (TSPC)

TSPC was monitored by utilizing the BCA protein assay kit from Thermo Scientific (Waltham, MA, USA) according to the manufacturer's protocol. Briefly, fifty (50) mg of watercress powder were measured and mixed thoroughly with 10 mL of double distilled water (ddH_20), vortexed, for 30 sec, and incubated at RT for 30 min. The resulting solution was centrifuged at 4,000 × *g*, for 10 min. The absorbance was measured at

562 nm and the results were normalized based on the (Bovine Serum Albumin) BSA standard curve created with a linear range of 0–2 mg/mL (R^2> 0.998). Data were expressed as means of mg of protein/mL/g of dry extract.

2.11. Determination of total soluble sugars content (TSSC)

Initially, fifty (50) mg of watercress powder was measured and mixed with 10 mL of double distilled water (ddH_20). Determination of TSSC was performed according to Kyriakou et al. (2022a). The absorbance was monitored at 490 nm and the results were calculated based on the mannose standard curve created with a linear range of 0-100 nM (R^2> 0.999). Data were expressed as means of nmol of mannose equivalents/g of dry extract.

2.12. Cell lines

The human malignant melanoma (A375) cell line was obtained from the American Type Culture Collection (ATCC, Manassas, VA, USA) whereas human metastatic malignant melanoma (Colo-679 and Colo-800) and epidermoid carcinoma (A431) cell lines were purchased from DSMZ (Braunschweig, Germany). Finally, the human immortalized keratinocyte (HaCaT) cell line was kindly provided by Dr Sharon Broby (Dermal Toxicology & Effects Group; Center for Radiation, Chemical and Environmental Hazards; Public Health England, Didcot, UK). A431, Colo-679 and Colo-800 cells were cultured in RPMI 1640 media while those of A375 and HaCaT in Dulbecco's Modified Eagle Medium (DMEM)-high glucose. All culture media were supplemented with 10% fetal bovine serum (FBS), 2 mM L-glutamine, and 1% Penicillin-Streptomycin (100 U/mL penicillin, 100 µg/mL streptomycin). Cells were grown as monolayer cultures in a humidified chamber at 37 °C and 5% CO_2 and subcultured when 80–90% confluency was reached for a maximum of 25 passages before new stocks were thawed and utilized.

2.13. Determination of cell viability by the Alamar blue assay

Overall, 8,000/4,000/2,000 A375 and A431 cells as well as 10000/5000/2500 Colo-679, Colo-800 and HaCaT cells per well were seeded (into 96-well plates) for 24, 48, and 72 hr, respectively. The following day, cells were treated with increasing concentrations *(% v/v)* of a watercress-derived PEITC enriched fraction (PhEF; at a final volume of 100 µL). At the end of all exposures, 10 µL of resazurin (1 mg/mL final concentration in PBS) was added directly to each well, mixed by gentle shaking and incubated in a humidified incubator at 37 °C/5% CO_2, for 4 hr. Finally, absorbance was measured at 570 nm and at 595 nm (reference wavelength) by utilizing a microplate reader (LT4500, Labtech, UK). Cell viability levels were calculated and expressed as percentage (%) of control (untreated) cells.

2.14. Exposure protocols

A375 cells were exposed to either single and/or combined treatments with (i) PhEF [1.5% *v/v*; calculated EC_{50} value] and/or (ii) apoptosome inhibitor NS3694 (20–100 µM). Specifically, A375 cells (4000 cells/well) were seeded into 96-well plates and left overnight to adhere, at 37^0C/5% CO_2. Next day, in single exposures, cells were either treated with PhEF (for 48 hr) or various concentrations (20–100 µM) of NS3694 apoptosome inhibitor (for 54 hr). In combined exposures, cells were initially pretreated with NS3694 inhibitor (for 6 hr) followed by incubations with 1.5% *v/v* of PhEF for additional 48 hr. After completion of all exposure protocols, cell viability levels were determined using the alamar blue assay, as previously described. Finally, for all immunoblotting experiments, 1.2×10^6 A375 cells were seeded in 100 mm plates and next day were pretreated with 20 µM of NS3694 inhibitor (for 6 hr) followed by exposures with 1.5% *v/v* of PhEF for a further 48 hr. At the end of incubations, cell pellets were collected and stored at −20 °C.

2.15. Determination of caspases-3, -8 and -9 activity levels

The fluorometric Caspases-3, −8 and −9 Multiplex Activity Assay Kit was utilized according to the manufacturer's instructions. Briefly, A375 cells (4,000 cells/well) were seeded in black, sterile 96-well plates and incubated in a humidified chamber at 37 °C, 5% CO_2. The following day, cells were treated with either 200 µM *tert*-Butyl hydroperoxide (TBH; used as positive control) or 1.5% *v/v* PhEF. At the end of incubations, 100 µL of caspase assay loading solution (50 µL of each caspase substrate mixed with 10 mL of assay buffer) were added directly to the culture medium and incubated for 1 hr, at RT, in dark. Caspase activity was monitored in a fluorescence microplate reader (Synergy H1, Bio-Tek, US) using the following wavelengths: Caspase 3: Ex/Em = 535/620 nm, Caspase 8: Ex/Em = 490/525 nm, Caspase 9: Ex/Em = 370/450 nm. Data were expressed as relative fluorescent units (RFU).

2.16. Quantitative real-time PCR (qRT-PCR)

Briefly, A375, Colo-679 and Colo-800 cells were seeded in a 100 mm plate overnight and next day were treated with their respective EC_{50} values over 48 hr. Then, RNA was extracted (utilizing the NucleoZol reagent) while its concentration and quality were determined by utilizing a NanoDrop™ One/OneC Microvolume UV-Vis Spectrophotometer (ThermoFisher Scientific, UK). For cDNA synthesis, the PrimeScript™ RT Reagent (Perfect Real Time) kit was used, and samples were stored at −20 °C, until further use. Real-time PCR experiments were performed in a StepOne™ Real-Time PCR instrument (Thermo Fisher Scientific, UK) using SYBR Green qPCR Master Mix (High ROX). Reaction mixtures contained 1 µg of cDNA, SYBR green PCR master mix and 10 µM of forward and reverse primers (Table S7, Supplementary Info) to a final volume of 20 µL. The qRT-PCR set up was as follows: Step 1 (95 °C for 3 min); Step 2 (40 cycles at 95 °C for 15 sec each); Step 3 (60 °C

for 1 min) whereas melt curve analysis was performed by heating for 1 hr at 95 °C. Finally, relative levels of gene expression were normalized to GAPDH using the ΔΔCt method. Data were expressed as fold changes compared to control.

2.17. Protein extraction and quantification

Following exposures, A375 cells were lysed with RIPA lysis buffer (150 mM sodium chloride, 50 mM Tris-HCl pH 8.0, 1% NP-40, 0.5% sodium deoxycholate, 0.1% SDS) supplemented with phosphatase/protease inhibitors. Lysates were incubated on ice and vortexed, every 10 min, for 30 min followed by centrifugation at 14,000 *x* g, for 15 min, at 4 °C until whole cell extracts (supernatants) were collected. Protein quantification was performed using the BCA protein assay kit according to manufacturer's instructions.

2.18. Western immunoblotting

Briefly, 80 µg of protein extracts were separated on FastGene PAGE precast gels (gradient: 4–20%, 10 × 8 cm) in a FastGene PAGE Protein System (Nippon Genetics, Düren, Germany). Separated proteins were then transferred to PVDF membranes (0.2 µm) using a Trans-Blot Turbo Transfer System (Bio-Rad Laboratories, UK). Then nonspecific sites of membranes were blocked either in 5% nonfat dry milk or 5% Bovine Serum Albumin (BSA) in TBST buffer (150 mM NaCl, 100 mM Tris pH 7.5, 0.1% *v/v* Tween-20), for 2 hr, at RT. Afterwards, membranes were incubated with the following primary antibodies: anti-Caspase-2 (1:1000), anti-caspase-9 (1:1000), anti-Bcl-XL (1:1000), anti-cytochrome c (1:1000), anti-Bax (1:1000), anti-FLIP (1:1000), anti-DCR2 (1:1000), anti-Bcl2 (1:1000), anti-GAPDH (6C6) (1:1000) and anti-β-actin (1:10 000), at 4 °C, overnight. The following day, membranes were washed three times with 1% TBST buffer [50 mM Tris, 150 mM NaCl, 0.1% *v/v* Tween-20] and incubated with secondary antibody (mouse or rabbit at 1:1000) at RT, for 1 hr, followed by three washes with 1% TBST. Finally, membrane bands were developed using the FUSION solo X imaging system (Vilber Lourmat, France). Immunoblots were stripped utilizing a stripping buffer [1.5% *w/v* glycine, 0.1% *w/v* SDS, 1% *v/v* Tween 20] and reprobed with the desired antibody. Densitometry was performed using the Image J software (1.44n, National Institute of Health, Bethesda, MD, USA). Data were normalized against either β-actin or GAPDH and were expressed as fold change from control.

2.19. Statistical analysis

Data were analyzed using the Microsoft Office Excel 2016 software and were expressed as mean values ± standard deviation (SD) from three independent experiments. Statistical analyses were performed by one-way ANOVA with Tukey's test for multiple comparisons and/or student's *t*-test by using Graph Pad Prism 6 (GraphPad Software, San Diego, CA, USA). Values of $p < 0.05$, $p < 0.01$ and $p < 0.001$ were considered as statistically significant.

3. Results

3.1. Chemical characterization of Nasturtium officinale (watercress) powder extract

3.1.1. Phytochemical content

Several methodologies were recruited for detecting and quantifying various phytochemicals in the watercress powder extract. Initially, we evaluated TSSC, TSPC, TPC, TFC and pigments (e.g. lycopene, chlorophylls -a and -b as well as β-carotene). Overall, the results have demonstrated the presence of phenols (42.00 ± 2.08 mg of GAE/g of dry extract) as well as flavonoids (73.77 ± 3.57 mg of RE and 17.18 ± 1.69 mg of CE/g of dry extract). Also, detection and analysis of pigments' content revealed the presence of lycopene (10.45 ± 2.36 mg of pigments/g of dry extract) and chlorophylls -A and -B (17.18 ± 1.69 and 34.93 ± 2.23 mg of pigments/g of dry extract, respectively). In fact, the content of chlorophyll -b was the most abundant while only traces of β-carotene (0.05 ± 0.02 mg of pigments/g of dry extract) were detected **(**Table 1**)**.

3.1.2. GL and ITC contents

We sought to detect and quantify GLs' and their respective ITCs' contents by utilizing a UPLC-ESI-MS/MS methodology. Considering the unstable nature of ITCs, due to their high volatility, their derivatization (excluding indole-3-carbinol) into the respective thiourea derivatives was essential. Overall, our findings revealed that the most abundant GLs were Gluconasturtiin (38.59 ± 1.12 ng/g of dry extract) and Glucobrassicin (19.22 ± 0.10 ng/g of dry extract). In contrast, Glucoiberin, Glucoraphanin, Glucoberteroin, Glucolimnanthin and 4-methoxyglucobrassicin were not detected in the watercress powder extract. On the other hand, the most abundant ITCs were PEITC (139.02 ± 0.36 ng/g of dry extract) followed by indole-3-carbinol (90.32 ± 0.81 ng/g of dry extract) while all others were either minimally detected (as traces) or their content was out of the limit of detection **(**Table 1**)**.

3.1.3. Polyphenol content

In another set of experiments, we aimed to determine the absolute values of each flavonoid and phenol compounds, in the watercress powder, by a UPLC - MS/MS approach. Our results showed increased concentrations of Quercetin-3-O-rutinoside (1185.86 ± 5.23 ng/g of dry extract) followed by 4-methoxy flavanone (512.00 ± 0.12 ng/g of dry extract) and ferulic acid (324.78 ± 2.44 ng/g of dry extract). Increased levels of isorhamnetin (176.24 ± 4.29 ng/g of dry extract) and protocatechuic acid (100.36 ± 1.12 ng/g of dry extract) were also observed. Alternatively, 4-hydroxybenzoic acid, 5-methoxyflavanone and ipriflavone appeared to be not detected (Table 1).

3.2. Biological characterization of watercress-derived PhEF

3.2.1. PhEF induces cytotoxicity in malignant melanoma cells

In this series of experiments, we assessed the cytotoxic efficacy of PhEF against an *in vitro* model of human malignant

Table 1. Detection and quantification of TPC, TFC, total soluble sugars, total soluble proteins, pigments, glucosinolates, polyphenols and ITCs.

Analyte	Content	Units
Polyphenols		
4-Hydroxybenzoic acid	n.d.	ng of Polyphenols/g of dry extract
Protocatechuic acid	100.36 ± 1.12	
Gallic acid	54.12 ± 1.62	
Vanillin	2.98 ± 0.09	
Syringic acid	4.21 ± 0.05	
P-coumaric acid	20.59 ± 1.12	
Caffeic acid	11.98 ± 0.28	
Ferulic acid	324.78 ± 2.44	
Rosmarinic acid	24.98 ± 0.42	
Chlorogenic acid	62.01 ± 0.18	
Ellagic acid	2.17 ± 0.21	
2-Hydroxyflavanone	33.04 ± 0.62	
7-Hydroxyflavanone	15.21 ± 0.50	
4-Methoxyflavanone	512.00 ± 0.12	
5-Methoxyflavanone	n.d.	
Apigenin-7-O-rhamnoside	4.02 ± 0.03	
Luteolin-7-O-rutinoside	6.84 ± 0.03	
Isorhamnetin	176.24 ± 4.29	
Quercetin-3-O-rhamnoside	1.99 ± 0.36	
Quercetin-3-O-rutinoside	1185.86 ± 5.23	
Hyperoside	81.25 ± 0.68	
Myricetin-3-O-galactoside	13.05 ± 0.23	
Kaempferol-3-O-rutinoside	9.57 ± 0.21	
Ipriflavone	n.d.	
Naringin	12.45 ± 0.03	
TPC	42.00 ± 2.08	mg of GAE/g of dry extract
TFC	73.77 ± 3.57	mg of RE/g of dry extract
	17.18 ± 1.69	mg of CE/g of dry extract
Pigment		
Lycopene	10.45 ± 2.36	mg of Pigments/g of dry extract
Chlorophyll-α	17.18 ± 1.69	
Chlorophyll-β	34.93 ± 2.23	
β-Carotene	0.05 ± 0.02	
TSSC	195.23 ± 8.56	nmol of ME/g of dry extract
TSPC	12.23 ± 0.02	mg/ml of BSAE/g of dry extract
Glucosinolates		
Glucoiberin	n.d.	ng Glucosinolates/g dry extract
Glucoraphanin	n.d.	
Glucocamelinin	9.32 ± 0.42	
Homoglucocamelinin	0.18 ± 0.03	
Glucoarabin	n.d.	
Glucoraphenine	4.22 ± 0.12	
Glucocheirolin	0.28 ± 0.01	
Glucolepidiin	7.98 ± 0.44	
Glucoberteroin	n.d.	
Glucoerucin	2.98 ± 0.12	
Sinigrin	0.20 ± 0.02	
Gluconapin	3.24 ± 0.16	
Glucobrassicanapin	0.05 ± 0.01	
Epiprogoitrin	0.45 ± 0.04	
Progoitrin	4.06 ± 0.01	
Glucolimnanthin	n.d.	
Sinalbin	0.02 ± 0.01	
Gluconasturtiin	38.59 ± 1.12	
Glucotropaeolin	5.98 ± 0.02	
Glucobrassicin	19.22 ± 0.10	
Glucomoringin	3.02 ± 0.10	
4-Methoxyglucobrassicin	n.d.	
Isothiocyanates		
Sulforaphane	n.d.	ng Isothiocyanates/g dry extract
Iberin	n.d.	
Benzyl isothiocyanate	0.28 ± 0.04	
Phenethyl isothiocyanate	139.02 ± 0.36	
Allyl isothiocyanate	0.65 ± 0.12	
Indole-3-carbinol	90.32 ± 0.81	

Data are means ± SD of three independent experiments; n.d.: non-detected.

melanoma consisting of malignant melanoma (A375, Colo-679 and Colo-800), non-melanoma epidermoid carcinoma (A431) and non-tumorigenic immortalized keratinocyte (HaCaT) cells. All cells were subjected to increasing concentrations of PhEF for 24-72 hr. Overall, our results indicated a dose- and time-dependent decrease of cell viability levels in all malignant melanoma cells, to a variable degree. On the other hand, non-melanoma cells appeared to be more resistant, as a significant decline of cell viability was observed only at high concentrations of PhEF (7.5% *v/v* for A431 cells and 25/50% *v/v* for HaCaT cells) or prolonged exposures (at 72 hr) (Figures 1(A–E)). Specifically, calculated EC_{50} values of PhEF followed a similar pattern in all malignant melanoma cells where A375 cells were the most sensitive followed by Colo-679 and Colo-800 cells (Figures 1(A–C) and Table 2). Although PhEF also induced significant cytotoxicity against A431 cells (at any time of exposure) they were shown to be more resistant when compared to the melanoma cells and especially A375 (Figure 1(D) and Table 2). Finally, PhEF was shown to exert no cytotoxicity against HaCaT cells except perhaps at very high concentrations (25–50% *v/v*) and very prolonged durations of exposure (Figure 1(E) and Table 2). To conclude, PhEF's EC_{50} value at 48 hr of exposure was selected as the optimum experimental condition in following up experiments for evaluating PhEF's anti-cancer potency against A375 cells as this cell line was shown to be the most sensitive one among all tested melanoma cell lines.

3.2.2. PhEF induces the activity of major apoptotic caspases in A375 cells

Next, we sought to determine the potential of PhEF to inducing apoptosis in A375 cells. Cells were exposed to 1.5% *v/v* PhEF, for 48 hr, during which the enzymatic activity levels of caspases −3/−8/−9 were determined. Briefly, the activity levels of caspases −8 and −9 (indicative of the activation of extrinsic and intrinsic apoptosis, respectively) were significantly increased with those of caspase −9 being at a much higher level compared to the ones of caspase −8 (Figure 2(Ai–ii)). Finally, the activity levels of execution caspase-3 were also increased however, to a lesser extent when compared to caspases −8 and −9 (Figure 2(Aiii)).

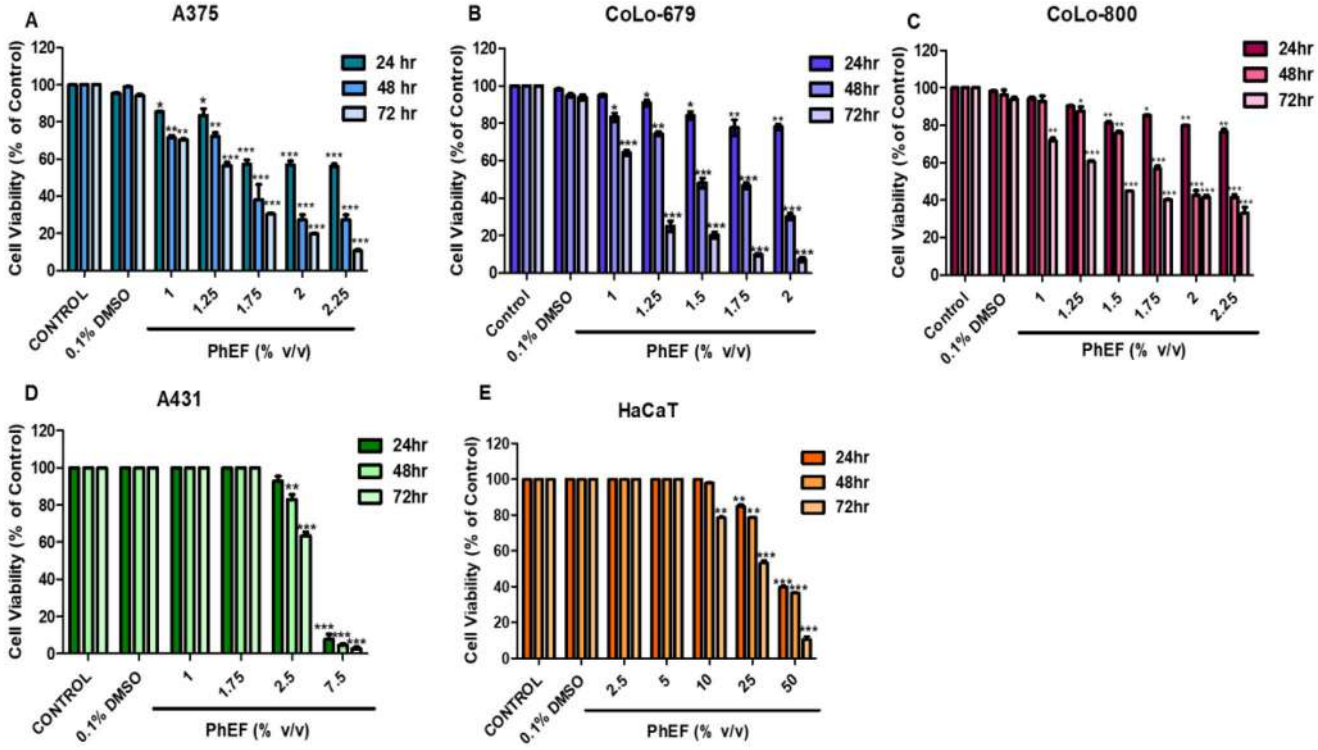

Figure 1. Cytotoxic profile of watercress-derived PhEF in an *in vitro* model of human malignant melanoma consisting of (A) A375, (B) Colo-679, (C) Colo-800 (malignant melanoma), (D) A431 (non-melanoma epidermoid carcinoma) and (E) HaCaT (nontumorigenic immortalized keratinocyte) cells. All cells were exposed to increasing concentrations of PhEF for 24, 48 and 72 hr. Data are expressed as means ± SEM and are representative of three independent experiments. Statistical significance was set at $*p < 0.05$, $**p < 0.01$, $***p < 0.001$ relative to 0.1% DMSO.

Table 2. Half maximal effective concentrations (EC_{50}; expressed as % *v/v)* of PhEF against A375, Colo-679, Colo-800, A431 and HaCaT cells following 24, 48, and 72 hr of exposure.

	A375	Colo-679	Colo-800	A431	HaCaT
Time (hr)			EC_{50} (% *v/v*)		
24	2.323 ± 0.343	3.329 ± 0.438	4.603 ± 0.279	4.399 ± 0.314	43.360 ± 0.083
48	1.526 ± 0.403	1.594 ± 0.385	1.818 ± 0.423	3.590 ± 0.536	40.580 ± 0.037
72	1.329 ± 0.159	1.086 ± 0.602	1.518 ± 0.194	2.522 ± 0.004	23.330 ± 0.296

Data are expressed as means ± SEM and are representative of three independent experiments. EC_{50} values were calculated through GraphPad software (version 5).

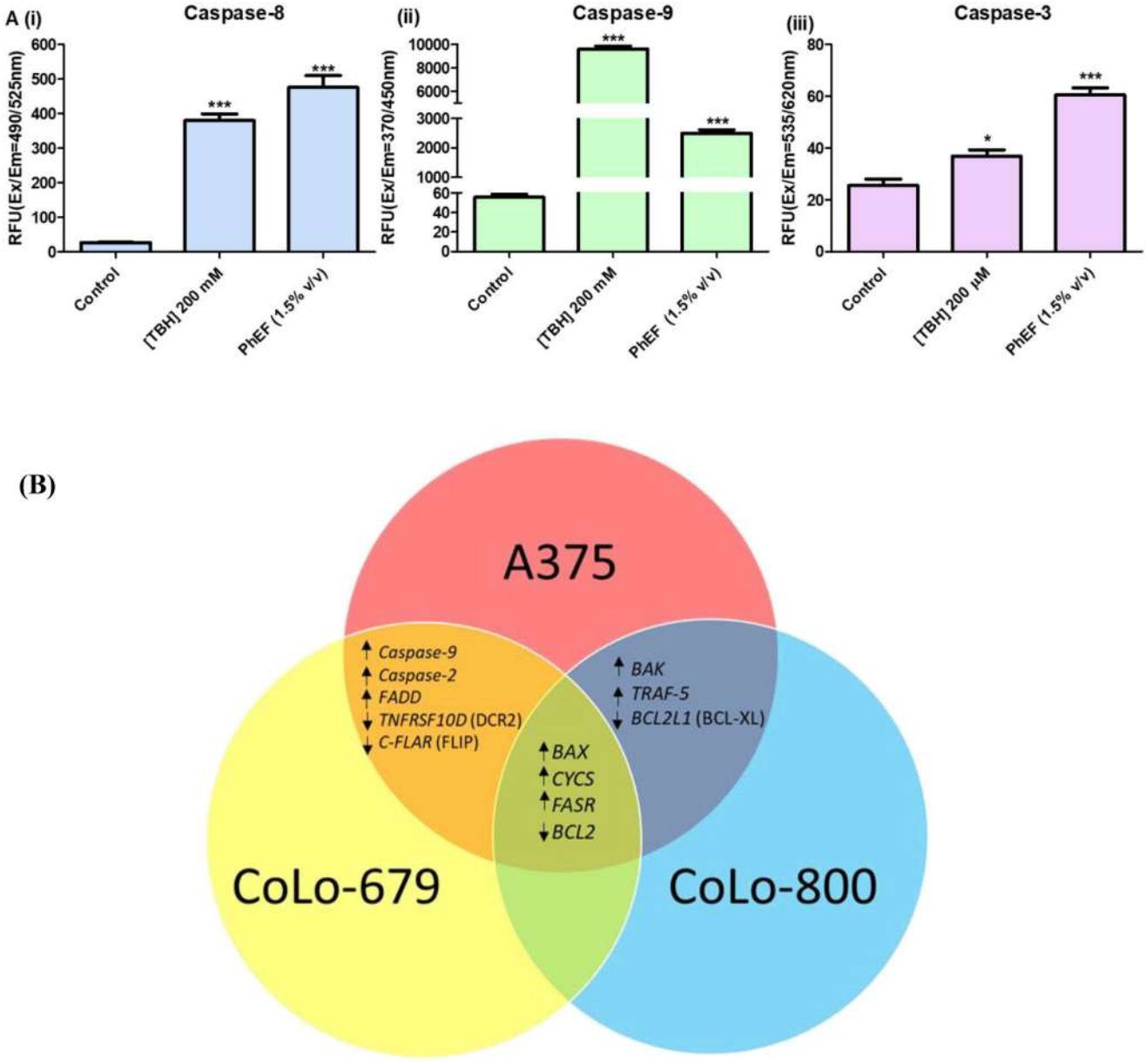

Figure 2. (A) Enzymatic activity levels of (i) Casp-8, (ii) Casp-9 and (iii) Casp-3 in A375 cells following exposure to 1.5% *v/v* PhEF, for 48 hr. Tert-butyl hydroperoxide (TBH; at 200 µM) was used as a positive control; (B) Differential expression patter of a panel of 12 apoptotic genes characterized by either up- (≥1.5-fold) or down-regulation (≤0.5-fold) in at least two of the three malignant melanoma cell lines. The purple panel indicates genes common in A375 and Colo-800 cells whereas orange indicates those being common in A375 and Colo-679 cells. Light green panel indicates genes common in all three cell lines. Data are expressed as means ± SEM and are representative of at least three independent experiments. Statistical significance was set at $^{*}p < 0.05$, $^{**}p < 0.01$, $^{***}p < 0.001$ relative to control.

3.2.3. PhEF induces the expression of key apoptotic genes in A375 cells

In an attempt to characterize the effect of PhEF in inducing apoptosis, several gene targets were evaluated known to regulate the apoptotic process. Specifically, the expression levels of various genes were assessed, upon the previously described experimental conditions, by utilizing a qRT-PCR approach. These genes were involved either in the intrinsic [*Casp-3, Casp-9, Apaf1, Bax, Bak, CYCS, Bid, Diablo, PMAIP 1 (Noxa), Casp-7, BCL2L11 (Bim), Casp-6*], extrinsic [*FASR, Traf2, Traf5, TNF, Casp-8, FASL, TNFRSF1A (TNFR), FADD, TRADD, TNFRSF10A (DR4), TNFRSF10 (TRAIL)*] apoptotic, anti-apoptotic [*(BCL2, MCL1, TNFRSF10D (DCR2), C-FLAR (FLIP), Bcl2l1 (BCL-XL), XIAP*] or other [*Casp-2, Casp-10*] pathways. Overall, 17 out of 31 genes were either up- (≥1.5-fold) or down-regulated (≤0.5-fold) in all three melanoma cell lines. Of these, a total of 12 genes exerted a similar gene expression profile in at least two out of the three melanoma cell lines. Specifically, four intrinsic (*BAX, BAK, Casp-9, CYCS*), three extrinsic (*FASR, TRAF-5, FADD*) and one other (*Casp-2*) genes exhibited at least 50% increase whereas four anti-apoptotic genes (*BCL2, TNFRSF10D, C-FLAR, BCL2L1*) showed 50% reduction in their expression levels (Tables S8–S9 and Figure S4, Supplementary Info). Finally, the distribution and overlap of these 12 genes was documented in all three malignant melanoma cell lines (Figure 2(B)).

3.2.4. PhEF induces intrinsic apoptosis and apoptosome formation in A375 cells

To further validate the effect of PhEF, in all 12 genes, western immunoblotting was performed for assessing their

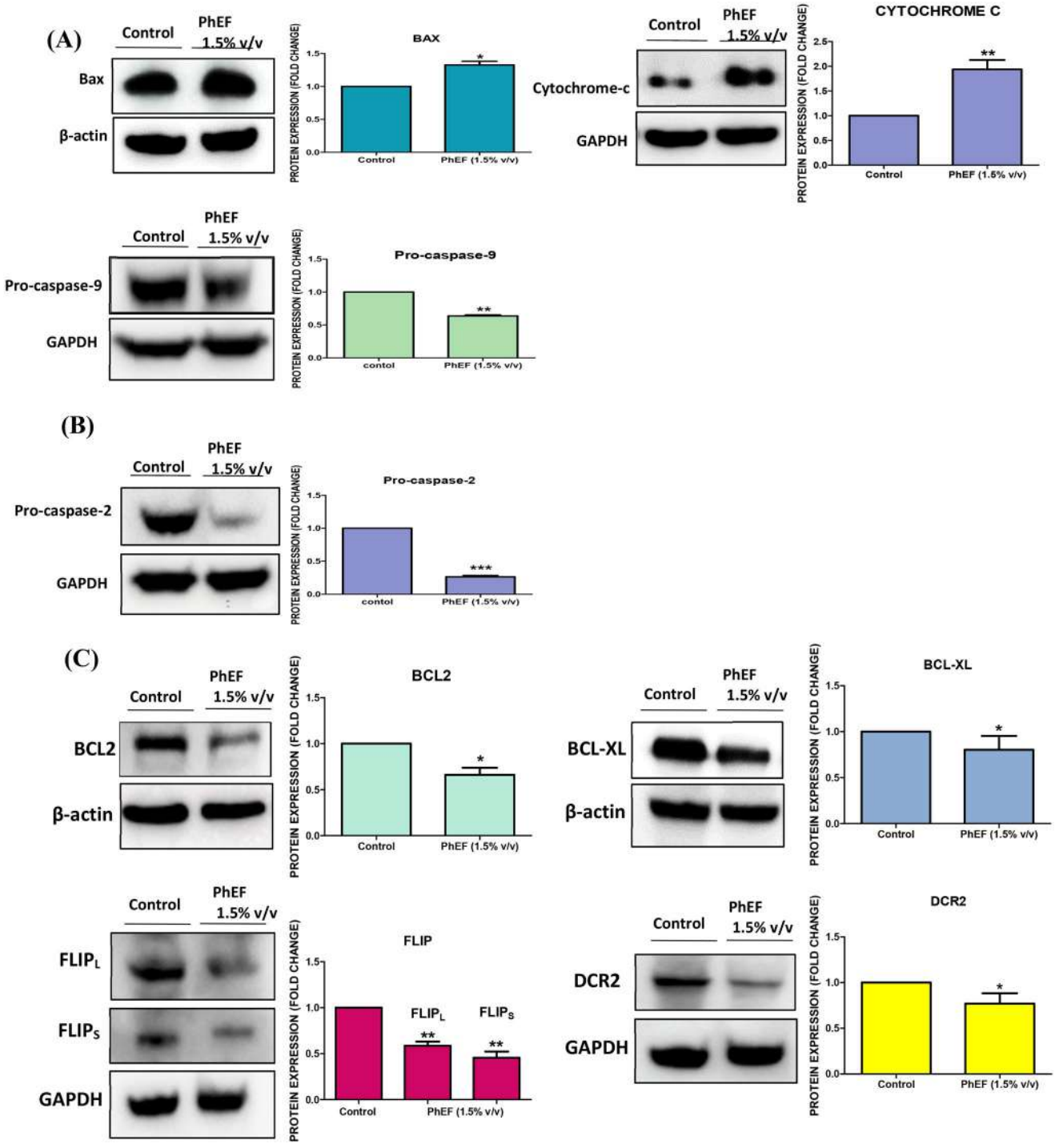

Figure 3. Activation of the intrinsic apoptotic Cascade upon treatment of A375 cells with 1.5%*v/v* PhEF, for 48 hr. Whole cell extracts were analyzed for (A) Bax, cytochrome C, Pro-caspase-9 (intrinsic pathway), (B) Caspase-2 and (C) BCL2, BCL-XCL, FLIP and DCR2 anti-apoptotic protein levels by Western immunoblotting. Equal protein loading was confirmed with either GAPDH or β-actin. Quantification of proteins was performed by densitometry. Data are expressed as means ± SEM of two independent experiments. Statistical significance was set at $*p < 0.05$, $**p < 0.01$, $***p < 0.001$ relative to control.

protein expression levels. Our results revealed that PhEF induced the activation of proteins involved in the intrinsic apoptotic pathway (Figure 3(A)) but had no effect in any of those involved in the extrinsic pathway (results not shown). In addition, there was significant inhibition of a number of anti-apoptotic proteins (Figure 3(C)). Specifically, we observed a significant up-regulation of the pro-apoptotic protein BAX along with a robust increase of cytochrome-c protein expression levels whereas pro-caspase −9 levels were decreased indicative of its cleavage to its active form (Figure 3(A)). To this end, pro-caspase −2 levels also exhibited marked reduction also indicative of its cleavage and activation (Figure 3(B)). Finally, protein expression levels of anti-apoptotic proteins Bcl-2, Bcl-XL, FLIP (FLIP$_L$ & FLIP$_S$) and DCR2 were all shown to be significantly inhibited (Figure 3(C)).

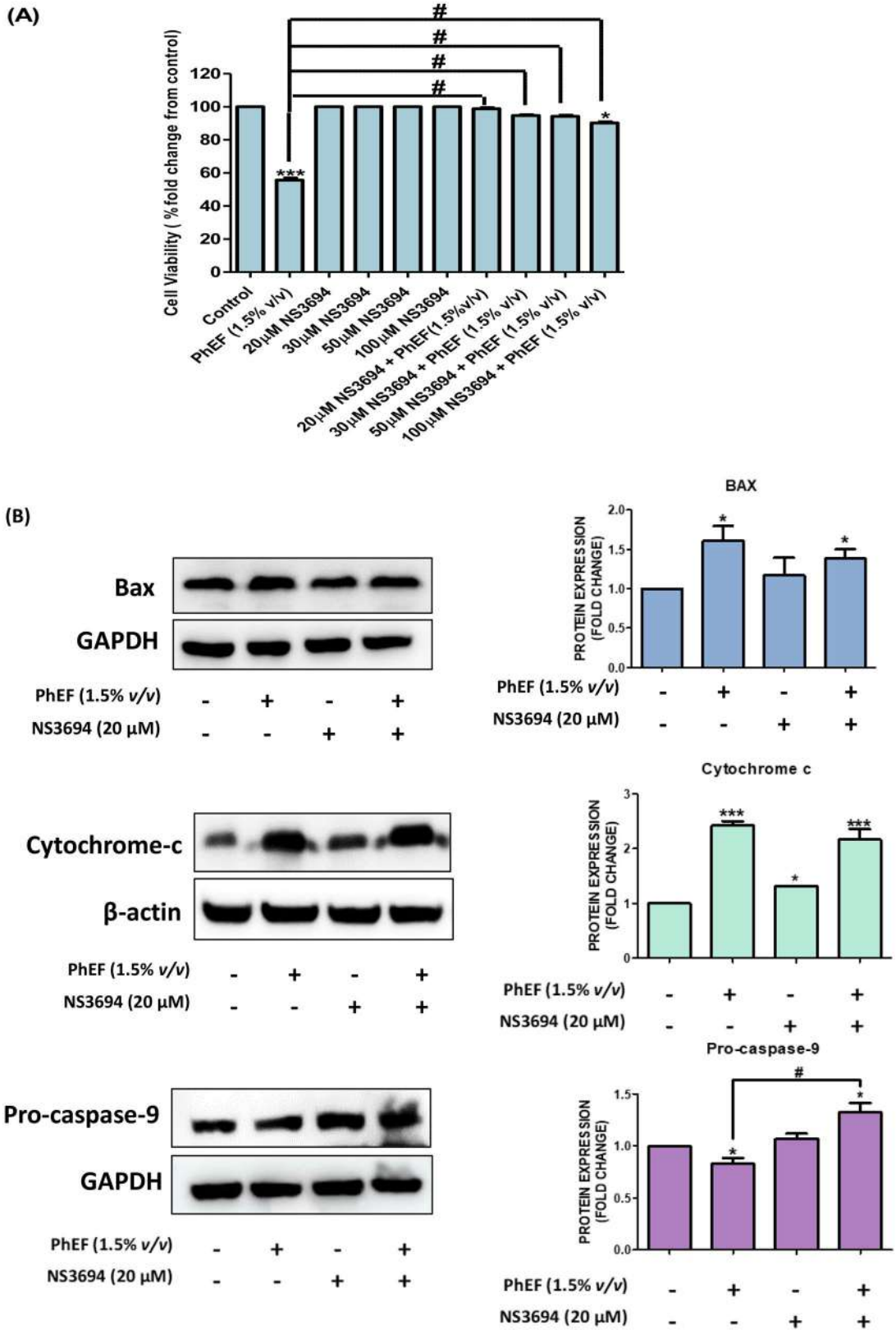

Figure 4. Apoptosome inhibitor NS3694, represses PhEF-induced apoptotic activation in A375 cells. (A) Cells were treated either with 1.5%*v/v* of PhEF, for 48h, or with increasing concentrations (20–100μM) of NS3694, for 6 hr, as single and combinatorial treatments, respectively. cell viability was monitored by the alamar blue assay; (B) Protein expression levels of Bax, cytochrome-c and pro-caspase-9 were assessed by Western immunoblotting. Equal protein loading was confirmed with either GAPDH or β-actin. Quantification of proteins was performed by densitometry Data are expressed as mean ± SEM of two independent experiments. Statistical significance was set at $^{*}p < 0.05$, $^{***}p < 0.001$ relative to control, $^{\#}p < 0.05$ relative to PhEF.

3.2.5. Apoptosome inhibitor NS3694 suppresses PhEF-induced activation of intrinsic apoptosis in A375 cells

To confirm our previous observations, A375 cells were exposed to increasing concentrations (20–100μM) of the apoptosome inhibitor NS3694 for 54 hr. Our data revealed that none of the tested concentrations of NS3694 affected

Table 3. List of clinical trials aiming to identify the biological benefit(s) of various isothiocyanates in different cancer types (source: ClinicalTrials.gov).

Intervention	Cancer type	Status	Phase	Identifier
PEITC (capsules)	Lung	Completed	Phase II	NCT00691132
PEITC (capsules)	Lung	Completed	Phase I	NCT00005883
Nutri-jelly with PEITC	Head & neck	Completed	N/A	NCT03034603
Allin and SFN	Prostate	Completed	N/A	NCT04046653
SFN-rich broccoli sprout extract capsules	Prostate	Completed	N/A	NCT01265953
SFN (tablets)	Prostate (recurrent)	Completed	Phase II	NCT01228084
High SFN extract (broccoli sprout extract)	Prostate	Completed	Phase I Phase II	NCT00946309
Standard broccoli soup/Beneforte® broccoli soup (glucoraphanin-enriched broccoli)/Beneforte® extra broccoli soup	Prostate	Completed	N/A	NCT01950143
BroccoMax® tablets (special blend of broccoli extract containing SFN)	Prostate	Active (not recruiting)	N/A	NCT03665922
Broccoli sprout extract	Breast	Completed	Phase II	NCT00982319
Broccoli sprout extract	Breast	Completed	Phase II	NCT00843167
SFN (tablets)	Lung	Completed	Phase II	NCT03232138
SFN (capsules)	Bladder	Withdrawn (grant not approved)	Phase II	NCT03517995
Broccoli sprout extract-SFN (capsules)	Atypical nevi-precursor melanoma lesions	Completed	Early phase I	NCT01568996
Broccoli sprout extract	Bladder	Terminated (low accrual)	N/A	NCT01108003
Broccoli sprout/broccoli seed extract (Avmacol®, extra strength)	Cigarette smoking-related carcinoma	Recruiting	Phase II	NCT05121051
Broccoli sprout/Broccoli seed extract (Avmacol®)	Tobacco-related carcinoma	Completed	Early phase I	NCT03402230
SFX-01 (synthetic sulforaphane stabilized by an alpha-cyclodextrin ring)/ Fulvestrant/Tamoxifen/Aromatase inhibitors	Breast (metastatic)	Completed	Phase II	NCT02970682
Brocoli sprout extract (Avmacol®)	Head & neck	Completed	Early phase I	NCT03182959
PEITC capsules	Lymphoproliferative	Withdrawn	Phase I	NCT00968461
Standard broccoli soup/Beneforte® extra broccoli soup (glucoraphanin-enriched broccoli)	Prostate	Terminated (issues with recruitment)	N/A	NCT02404428
Verum, broccoli sprout grain (capsules)	Pancreatic (advanced)	Unknown	N/A	NCT01879878

N/A: not applicable; PEITC: phenethyl isothiocyanate; SFN: sulphoraphane.

the viability of A375 cells (Figure 4(A)). Moreover, pretreatment with any concentration of NS3694, for 6 hr, followed by treatment with 1.5%*v/v* of PhEF, for an additional 48 hr, caused inhibition of PhEF-induced cytotoxicity (Figure 4(A)). Thus, pre-incubation with 20 µM of NS3694, for 6 hr, was chosen as the optimal experimental condition in all co-treatment experiments. Last, we assessed the effect of combined treatments on the expression levels of proteins involved in the formation of the apoptosome namely Bax, cytochrome c and pro-caspase 9. Our data revealed no significant effect in protein expression levels of Bax and cytochrome c between PhEF-treated cells in the absence or presence of NS3694. Finally, protein expression levels of pro-caspase-9 were significantly increased in the presence of NS3694, a finding which might indicate the accumulation of this caspase and ultimately its inability to convert into its active form and thereby not being able to participate in apoptotic induction (Figure 4(B)).

4. Discussion

In the present study, we aimed to determine the chemical composition of a lyophilized organic watercress powder in addition to determine the underlying mechanism(s) of its anticancer potency against an *in vitro* model of human malignant melanoma. Initially, our data revealed the presence of key phytochemicals, including phenolics, flavanols, soluble sugars and proteins, various pigments as well as specific GLs and corresponding ITCs. Our results are in agreement with previous reports, indicating the presence of various other phytochemicals, besides the presence of high amounts of PEITC (Rodrigues et al. 2016; Kyriakou et al. 2022a, 2022c). The increased volatility and the unstable nature of ITCs rendered their derivatization, into thiourea derivatives, essential for further analysis (Kyriakou et al. 2022c). To this end, our results showed that gluconasturtiin and its respective ITC namely PEITC to be the most abundant compounds. A finding also in agreement with previously published data (Jeon et al. 2017; Kyriakou et al. 2022b). Furthermore, our data also indicated increased levels of glucobrassicin and indole-3-carbinol in addition to other abundant polyphenols such as protocatechuic acid, isorhamnetin, 4-methoxyflavanone, quersetin-3-*O*-rutinoside and ferulic acid all of which agree with previously published work by our group (Kyriakou et al. 2022b). Last, a significant content of soluble sugars was detected for which previous reports have demonstrated to be essential in maintaining the intracellular redox balance of the plant while also facilitating its growth and metabolism. Specifically, soluble sugars have a crucial role in plant anabolism and catabolism by acting either as ROS scavengers or producers (Rosa et al. 2009; Sami et al. 2016; Kyriakou et al. 2022a). Similarly, the presence of a variety of pigments was observed which are known as plant's secondary metabolites and are essential for its growth, metabolism and

photosynthesis (Lu et al. 2021). To this end, we detected chlorophylls-α and -β as well as lycopene and β-carotenoids. Finally, chlorophylls are widely known for their antioxidant capacity by acting as ROS scavengers (Pérez-Gálvez et al. 2020; Cvitković et al. 2021).

In an attempt to delineate the anticancer potency of a watercress-derived PhEF extract, time- and dose-dependent kinetic experiments were performed showing a decline in cell viability levels in melanoma cell lines. On the other hand, moderate cytotoxicity was observed in epidermoid carcinoma cells but at higher EC_{50} values when compared to melanoma cells indicative of their resistance to PhEF-induced cytotoxicity. Finally, normal keratinocyte cells showed much higher levels of resistance to PhEF-induced cytotoxicity when compared to either malignant melanoma or epidermoid carcinoma cells. In this context, other reports have documented watercress-induced cytotoxicity in other types of cancer cell lines including those of breast, lung and colorectal origin (Giallourou et al. 2019; Adlravan et al. 2021; Taghavinia et al. 2022). On the other hand, a number of studies have demonstrated that ITCs (especially PEITC) can induce apoptosis in cancer cells by involving a plurality of mechanisms underlying various cellular cascades including intrinsic apoptosis, p53 signaling, epigenetic regulation, etc., (Mitsiogianni et al. 2018, 2021; Mitra et al. 2022). In a recent study, the authors have shown that PEITC can activate extrinsic pathways in glioblastoma cells by increasing caspase-3 and Bax protein levels while subsequently reducing Mcl-1 and XIAP anti-apoptotic protein levels thereby inhibiting tumor growth (Chou et al. 2017). Another study also revealed that an ITC-rich broccoli extract activated intrinsic apoptosis in human bladder cells by inducing increased DNA fragmentation together with loss of mitochondrial membrane potential thus leading to increased caspases −9 and −3 activity levels (Tang et al. 2006). Similarly, exposures of human malignant melanoma (A375) cells to synthetic PEITC resulted in apoptotic induction through activation of caspases −9, −3 and −6 (Mantso et al. 2016) whereas their exposure to a naturally-derived PEITC-enriched extract caused mitochondrial morphological changes and membrane depolarization resulting in the activation of caspases −9 and-3 (Kyriakou et al. 2023).

Next, we sought to investigate further into potential targets capable of regulating PhEF-induced apoptosis in human malignant melanoma cell lines. Our data revealed that PhEF induced the activation of caspase-9 (a marker of intrinsic apoptosis) at much higher levels than those of caspases −8 (a marker of extrinsic apoptosis) and −3 (a marker of execution apoptosis). Then, we investigated into the expression profile of 31 genes being either directly implicated in intrinsic and/or extrinsic apoptosis as well as in various anti-apoptotic mechanism(s). Our initial analysis revealed a panel of 17 genes being either up- and/or down-regulated of which, only 12 were validated in at least two out of the three of tested human malignant melanoma cell lines. Overall, our data showed that eight pro-apoptotic genes (*Caspases −9*, *−2*, *FADD*, *BAX*, *CYCS*, *FASR*, *BAK* and *TRAF5*) increased their expression levels by ≥ 1.5-fold whereas the remaining four anti-apoptotic genes (*TNFRSF10D*, *c-FLAR*, *BCL2* and *BCL2L11*) reduced decreased their expression levels by ≥0.5-fold. Finally, western immunoblotting analysis revealed that only eight of them were validated: procaspase-9, cytochrome c and Bax (implicated in intrinsic apoptosis), Bcl-2, Bcl-XL, FLIP and DCR2 (implicated in various anti-apoptotic mechanisms) and procaspase-2 (implicated in other apoptotic cascades). On the contrary, we did not observe any significant changes in protein expression levels of any member of the extrinsic apoptotic cascade thereby suggesting the activation of intrinsic apoptosis as the main mechanism of PhEF-induced cell death. Indeed, pre-exposures of A375 melanoma cells with the apoptosome inhibitor NS3694 resulted in complete inhibition of PhEF-induced cytotoxicity. As such, NS3694 significantly increased procaspase-9 protein expression levels, in co-treatment with PhEF, while Bax and cytochrome c levels remained largely unaffected. These results suggest that N3694 inhibited procaspase-9 cleavage into its active form thus preventing PhEF-induced apoptotic activation. In fact, others have shown that NS3694 specifically suppresses cytochrome c-induced formation of apoptosome complex by blocking the activation of the initiator caspase-9, thus inhibiting mitochondria-mediated apoptosis (Lademann et al. 2003). Overall, our data suggest that PhEF is a potent anti-melanoma agent via its capacity to induce the activation of the intrinsic (mitochondrial) apoptotic pathway.

Finally, several clinical trials, using mainly PEITC, SFN and broccoli sprout extracts (BSE), have been conducted in patients with lung, head and neck, prostate, breast, bladder, lymphoproliferative and pancreatic cancers **(**Table 3**)**. However, the majority of these trials have produced contradictory results either associated with an important clinical benefit or a limited anti-cancer efficacy, depending on the type of cancer. For instance, administration of a Nutri-PEITC jelly formulation (containing 20 mg of PEITC) in patients with advanced oropharyngeal cancer (NCT03034603) was shown to increase serum levels of *p53*, stabilize the progress of the disease and improve the overall patient's quality of life (Lam-Ubol et al. 2023). On the other hand, PEITC supplementation in smokers (NCT00691132) was shown to act as an important inhibitor of lung carcinogenesis through metabolic modulation of 4-(methylnitrosamino)-1-(3-pyridyl)-1-butanone (NNK); a known tobacco carcinogen (Yuan et al. 2016). Another clinical study (NCT01228084) indicated that although the administration of SFN-rich extracts to patients with recurrent prostate cancer was safe, there was significant lengthening of the on-treatment prostate specific antigen (PSA) doubling time (PSADT) compared to that before treatment (Alumkal et al. 2015). In parallel, daily administration of SFN-rich broccoli sprout extract capsules in patients scheduled for prostate biopsy (NCT01265953), indicated a potential preventive mechanism against disease onset through downregulation of *AMACR* and *ARLNC1* genes associated with the development of prostate carcinoma (Zhang et al. 2020). Interestingly, the number of ITCs-related clinical trials in melanoma patients is rather limited. However, in a pilot study (NCT01568996), administration of BSE-SFN capsules (50–200μmol) in melanoma patients was well tolerated and a gradual dose-dependent increase of both skin and plasma SFN levels was observed together with alterations in inflammatory

cytokines and tumor suppressor *decorin* expression levels (Tahata et al. 2018). Despite the number of ITCs-related clinical trials, against different cancer types, their use in the clinical practice is rather limited and still controversial. In fact, a variety of factors such as their low aqueous solubility, chemical instability, low bioavailability and limited efficacy in overcoming biological barriers and penetrating into solid tumors, recapitulate, at least in part, their limited success in clinical trials as opposed to pre-clinical models (Na et al. 2023).

4.1. Study limitations

Although our current data provide evidence of an anti-melanoma activity of PhEF, further experiments are required in order to better characterize and further validate the role of apoptosome formation as an underlying molecular mechanism involved in the action of PhEF against the other human malignant melanoma (Colo-679 and Colo-800) cell lines. This is of particular importance as we have previously demonstrated that the cytotoxic effect of PhEF against malignant melanoma cell lines is not attributed to the activity of PEITC itself but rather on its *N*-acetyl conjugated form thereby providing further insights into the plausible mode of action of naturally-derived PEITC (Kyriakou et al. 2024). In addition, only recently, it was shown that many types of phytochemicals (including ITCs) can exhibit a hormetic effect descriptive of their capacity to either promote or inhibit tumor growth at their low or high concentrations, respectively (Bao et al. 2014; Singh et al. 2019). Moreover, physicochemical parameters such as low rates of solubility, stability and bioavailability remain challenging to overcome due to the chemical nature of ITCs thus, partially, contributing to the lack of translation of *in vitro* results to *in vivo* systems (Bao et al. 2014; Oliviero et al. 2018; Singh et al. 2019). For the above reasons, there is a great need for further optimization of experimental protocols, along with the use of more sophisticated delivery systems (e.g. nanoparticles), in order to overcome physicochemical barriers and ultimately increase therapeutic efficacy.

Acknowledgments

The human immortalized keratinocyte (HaCaT) cell line was kindly provided by Dr. Sharon Broby (Dermal Toxicology & Effects Group; Centre for Radiation, Chemical and Environmental Hazards; Public Health England, Didcot, UK).

Disclosure statement

No potential conflict of interest was reported by the author(s).

Funding

This research was funded by a grant provided by the (i) Cyprus Institute of Neurology and Genetics, Nicosia, Cyprus under Telethon Cyprus (M.I.P.), (ii) Hellenic Foundation for Research and Innovation (H.F.R.I.) under the 'First call for H.F.R.I. research projects to support faculty members and researchers and the procurement of high-cost research equipment; Project Number: HFRI-FM17C3-2007' (A.P and M.I.P) and (iii) 'OPENSCREEN-GR: An Open-Access Research Infrastructure of Target-Based Screening Technologies and Chemical Biology for Human and Animal Health, Agriculture and Environment' [MIS 5002691] which is implemented under the Action 'Reinforcement of the Research and Innovation Infrastructure', funded by the Operational Programme 'Competitiveness, Entrepreneurship and Innovation' [NSRF 2014-2020] and co-financed by Greece and the European Union (European Regional Development Fund) (A.P.).

Data availability statement

All data generated and analyzed in this work are included in this manuscript. Additional data are freely available in the Supplementary materials section.

References

Adlravan E, Nejati K, Karimi MA, Mousazadeh H, Abbasi A, Dadashpour M, Sepideh jalilzadeh-Razin. 2021. Potential activity of free and PLGA/PEG nanoencapsulated nasturtium officinale extract in inducing cytotoxicity and apoptosis in human lung carcinoma A549 cells. J Drug Deliv Sci Technol. 61:102256. doi: 10.1016/j.jddst.2020.102256.

Alqathama A. 2020. BRAF in malignant melanoma progression and metastasis: potentials and challenges. Am J Cancer Res. 10(4):1103–1114.

Alumkal JJ, Slottke R, Schwartzman J, Cherala G, Munar M, Graff JN, Beer TM, Ryan CW, Koop DR, Gibbs A, et al. 2015. A phase II study of sulforaphane-rich broccoli sprout extracts in men with recurrent prostate cancer. Invest New Drugs. 33(2):480–489. doi: 10.1007/s10637-014-0189-z.

Anestopoulos I, Kyriakou S, Tragkola V, Paraskevaidis I, Tzika E, Mitsiogianni M, Deligiorgi MV, Petrakis G, Trafalis DT, Botaitis S, et al. 2022. Targeting the epigenome in malignant melanoma: facts, challenges and therapeutic promises. Pharmacol Ther. 240:108301. doi: 10.1016/j.pharmthera.2022.108301.

Bao Y, Wang W, Zhou Z, Sun C. 2014. Benefits and risks of the hormetic effects of dietary isothiocyanates on cancer prevention. PLOS One. 9(12):e114764. doi: 10.1371/journal.pone.0114764.

Barba FJ, Nikmaram N, Roohinejad S, Khelfa A, Zhu Z, Koubaa M. 2016. Bioavailability of glucosinolates and their breakdown products: impact of processing. Front Nutr. 3:24. doi: 10.3389/fnut.2016.00024.

Bolick NL, Geller AC. 2021. Epidemiology of melanoma. Hematol Oncol Clin North Am. 35(1):57–72. doi: 10.1016/j.hoc.2020.08.011.

Boyd LA, McCann MJ, Hashim Y, Bennett RN, Gill CIR, Rowland IR. 2006. Assessment of the anti-genotoxic, anti-proliferative, and anti-metastatic potential of crude watercress extract in human colon cancer cells. Nutr Cancer. 55(2):232–241. doi: 10.1207/s15327914nc5502_15.

Chen C-Y, Kao C-L, Liu C-M. 2018. The cancer prevention, anti-inflammatory and anti-oxidation of bioactive phytochemicals targeting the TLR4 signaling pathway. Int J Mol Sci. 19(9):2729. doi: 10.3390/ijms19092729.

Chikara S, Nagaprashantha LD, Singhal J, Horne D, Awasthi S, Singhal SS. 2018. Oxidative stress and dietary phytochemicals: role in cancer chemoprevention and treatment. Cancer Lett. 413:122–134. doi: 10.1016/j.canlet.2017.1.

Chou Y-C, Chang M-Y, Wang M-J, Liu H-C, Chang S-J, Harnod T, Hung C-H, Lee H-T, Shen C-C, Chung J-G. 2017. Phenethyl isothiocyanate alters the gene expression and the levels of protein associated with cell cycle regulation in human glioblastoma GBM 8401 cells. Environ Toxicol. 32(1):176–187. doi: 10.1002/tox.22224.

Cvitković D, Lisica P, Zorić Z, Repajić M, Pedisić S, Dragović-Uzelac V, Balbino S. 2021. Composition and antioxidant properties of pigments of Mediterranean herbs and spices as affected by different extraction methods. Foods. 10(10):2477. doi: 10.3390/foods10102477.

Esfahani K, Roudaia L, Buhlaiga N, Del Rincon SV, Papneja N, Miller WH. 2020. A review of cancer immunotherapy: from the past, to the present, to the future. Curr Oncol. 27(Suppl 2):S87–S97. doi: 10.3747/co.27.5223.

Giallourou NS, Rowland IR, Rothwell SD, Packham G, Commane DM, Swann JR. 2019. Metabolic targets of watercress and PEITC in MCF-7 and MCF-10A cells explain differential sensitisation responses to ionising radiation. Eur J Nutr. 58(6):2377–2391. doi: 10.1007/s00394-018-1789-8.

Huang AC, Zappasodi R. 2022. A decade of checkpoint blockade immunotherapy in melanoma: understanding the molecular basis for immune sensitivity and resistance. Nat Immunol. 23(5):660–670. doi: 10.1038/s41590-022-01141-1.

Jeon J, Bong SJ, Park JS, Park Y-K, Arasu MV, Al-Dhabi NA, Park SU. 2017. De novo transcriptome analysis and glucosinolate profiling in watercress (*Nasturtium officinale* R. Br.). BMC Genomics. 18(1):401. doi: 10.1186/s12864-017-3792-5.

Kyriakou S, Tragkola V, Alghol H, Anestopoulos I, Amery T, Stewart K, Winyard PG, Trafalis DT, Franco R, Pappa A, et al. 2022a. Evaluation of bioactive properties of lipophilic fractions of edible and non-edible parts of *Nasturtium officinale* (watercress) in a model of human malignant melanoma cells. Pharmaceuticals. 15(2):141. doi: 10.3390/ph15020141.

Kyriakou S, Michailidou K, Amery T, Stewart K, Winyard PG, Trafalis DT, Franco R, Pappa A, Panayiotidis MI. 2022b. Polyphenolics, glucosinolates and isothiocyanates profiling of aerial parts of *Nasturtium officinale* (Watercress). Front Plant Sci. 13:998755. doi: 10.3389/fpls.2022.998755.

Kyriakou S, Trafalis DT, Deligiorgi MV, Franco R, Pappa A, Panayiotidis MI. 2022c. Assessment of methodological pipelines for the determination of isothiocyanates derived from natural sources. Antioxidants. 11(4):642. doi: 10.3390/antiox11040642.

Kyriakou S, Potamiti L, Demosthenous N, Amery T, Stewart K, Winyard PG, Franco R, Pappa A, Panayiotidis MI. 2023. A naturally derived watercress flower-based phenethyl isothiocyanate-enriched extract induces the activation of intrinsic apoptosis via subcellular ultrastructural and Ca2+ efflux alterations in an *in vitro* model of human malignant melanoma. Nutrients. 15(18):4044. doi: 10.3390/nu15184044.

Kyriakou S, Demosthenous N, Amery T, Stewart KJ, Winyard PG, Franco R, Pappa A, Panayiotidis MI. 2024. Naturally derived phenethyl isothiocyanate modulates induction of oxidative stress via its N-acetylated cysteine conjugated form in malignant melanoma. Antioxidants. 13(1):82. doi: 10.3390/antiox13010082.

Lademann U, Cain K, Gyrd-Hansen M, Brown D, Peters D, Jäättelä M. 2003. Diarylurea compounds inhibit caspase activation by preveting the formation of the active 700-kilodalton apoptosome complex. Mol Cell Biol. 23(21):7829–7837. doi: 10.1128/MCB.23.21.7829-7837.2003.

Lam-Ubol A, Sukhaboon J, Rasio W, Tupwongse P, Tangshewinsirikul T, Trachootham D. 2023. Nutri-PEITC jelly significantly improves progression-free survival and quality of life in patients with advanced oral and oropharyngeal cancer: a blinded randomized placebo-controlled trial. Int J Mol Sci. 24(9):7824. doi: 10.3390/ijms24097824.

Lu W, Shi Y, Wang R, Su D, Tang M, Liu Y, Li Z. 2021. Antioxidant activity and healthy benefits of natural pigments in fruits: a review. Int J Mol Sci. 22(9):4945. doi: 10.3390/ijms22094945.

Mantso T, Sfakianos AP, Atkinson A, Anestopoulos I, Mitsiogianni M, Botaitis S, Perente S, Simopoulos C, Vasileiadis S, Franco R, et al. 2016. Development of a novel experimental in vitro model of isothiocyanate-induced apoptosis in human malignant melanoma cells. Anticancer Res. 36(12):6303–6309. doi: 10.21873/anticanres.11226.

Mitra S, Emran TB, Chandran D, Zidan BMRM, Das R, Mamada SS, Masyita A, Salampe M, Nainu F, Khandaker MU, et al. 2022. Cruciferous vegetables as a treasure of functional foods bioactive compounds: targeting p53 family in gastrointestinal tract and associated cancers. Front Nutr. 9:951935. doi: 10.3389/fnut.2022.951935.

Mitsiogianni M, Amery T, Franco R, Zoumpourlis V, Pappa A, Panayiotidis MI. 2018. From chemo-prevention to epigenetic regulation: the role of isothiocyanates in skin cancer prevention. Pharmacol Ther. 190:187–201. doi: 10.1016/j.pharmthera.2018.06.001.

Mitsiogianni M, Koutsidis G, Mavroudis N, Trafalis DT, Botaitis S, Franco R, Zoumpourlis V, Amery T, Galanis A, Pappa A, et al. 2019. The role of isothiocyanates as cancer chemo-preventive, chemo-therapeutic and anti-melanoma agents. Antioxidants. 8(4):106. doi: 10.3390/antiox8040106.

Mitsiogianni M, Kyriakou S, Anestopoulos I, Trafalis DT, Deligiorgi MV, Franco R, Pappa A, Panayiotidis MI. 2021. An evaluation of the anti-carcinogenic response of major isothiocyanates in non-metastatic and metastatic melanoma cells. Antioxidants. 10(2):284. doi: 10.3390/antiox10020284.

Na G, He C, Zhang S, Tian S, Bao Y, Shan Y. 2023. Dietary isothiocyanates: novel insights into the potential for cancer prevention and therapy. Int J Mol Sci. 24(3):1962. doi: 10.3390/ijms24031962.

Narbad A, Rossiter JT. 2018. Gut glucosinolate metabolism and isothiocyanate production. Mol Nutr Food Res. 62(18):e1700991. doi: 10.1002/mnfr.201700991.

Oliviero T, Lamers S, Capuano E, Dekker M, Verkerk R. 2018. Bioavailability of isothiocyanates from broccoli sprouts in protein, lipid, and fiber gels. Mol Nutr Food Res. 62(18):e1700837. doi: 10.1002/mnfr.201700837.

Pereira LP, Silva P, Duarte M, Rodrigues L, Duarte CMM, Albuquerque C, Serra AT. 2017. Targeting colorectal cancer proliferation, stemness and metastatic potential using brassicaceae extracts enriched in isothiocyanates: a 3D cell model-based study. Nutrients. 9(4):368. doi: 10.3390/nu9040368.

Pérez-Gálvez A, Viera I, Roca M. 2020. Carotenoids and chlorophylls as antioxidants. Antioxidants. 9(6):505. doi: 10.3390/antiox9060505.

Rosa M, Prado C, Podazza G, Interdonato R, González JA, Hilal M, Prado FE. 2009. Soluble sugars – metabolism, sensing and abiotic stress: a complex network in the life of plants. Plant Signal Behav. 4(5):388–393. doi: 10.4161/psb.4.5.8294.

Rose P, Huang Q, Ong CN, Whiteman M. 2005. Broccoli and watercress suppress matrix metalloproteinase-9 activity and invasiveness of human MDA-MB-231 breast cancer cells. Toxicol Appl Pharmacol. 209(2):105–113. doi: 10.1016/j.taap.2005.04.010.

Rodrigues L, Silva I, Poejo J, Serra AT, Matias AA, Simplício AL, Bronze MR, Duarte CMM. 2016. Recovery of antioxidant and antiproliferative compounds from watercress using pressurized fluid extraction. RSC Adv. 6(37):30905–30918. doi: 10.1039/C5RA28068K.

Sami F, Yusuf M, Faizan M, Faraz A, Hayat S. 2016. Role of sugars under abiotic stress. Plant Physiol Biochem. 109:54–61. doi: 10.1016/j.plaphy.2016.09.005.

Shakour ZT, Shehab NG, Gomaa AS, Wessjohann LA, Farag MA. 2022. Metabolic and biotransformation effects on dietary glucosinolates, their bioavailability, catabolism and biological effects in different organisms. Biotechnol Adv. 54:107784. doi: 10.1016/j.biotechadv.2021.107784.

Sikorska-Zimny K, Beneduce L. 2021. The metabolism of glucosinolates by gut microbiota. Nutrients. 13(8):2750. doi: 10.3390/nu13082750.

Singh VK, Arora D, Ansari MI, Sharma PK. 2019. Phytochemicals based chemopreventive and chemotherapeutic strategies and modern technologies to overcome limitations for better clinical applications. Phytother Res. 33(12):3064–3089. doi: 10.1002/ptr.6508.

Taghavinia F, Teymouri F, Farokhrouz F, Bagherabad EH, Farjami S, Karimi E, Oskoueian E, Le HH, Shakeri M. 2022. Nanoliposome-loaded phenolics from nasturtium officinale improves health parameters in a colorectal cancer mouse model. Animals. 12(24):3492. doi: 10.3390/ani12243492.

Tahata S, Singh SV, Lin Y, Hahm ER, Beumer JH, Christner SM, Rao UN, Sander C, Tarhini AA, Tawbi H, et al. 2018. Evaluation of biodistribution of sulforaphane after administration of oral broccoli sprout extract in melanoma patients with multiple atypical nevi. Cancer Prev Res. 11(7):429–438. doi: 10.1158/1940-6207.CAPR-17-0268.

Tang L, Zhang Y, Jobson HE, Li J, Stephenson KK, Wade KL, Fahey JW. 2006. Potent activation of mitochondria-mediated apoptosis and arrest in S and M phases of cancer cells by a broccoli sprout extract. Mol Cancer Ther. 5(4):935–944. doi: 10.1158/1535-7163.MCT-05-0476.

Yuan J-M, Stepanov I, Murphy SE, Wang R, Allen S, Jensen J, Strayer L, Adams-Haduch J, Upadhyaya P, Le C, et al. 2016. Clinical trial of 2-phenethyl isothiocyanate as an inhibitor of metabolic activation of a tobacco-specific lung carcinogen in cigarette smokers. Cancer Prev Res. 9(5):396–405. doi: 10.1158/1940-6207.CAPR-15-0380.

Zhang Y. 2012. The molecular basis that unifies the metabolism, cellular uptake and chemopreventive activities of dietary isothiocyanates. Carcinogenesis. 33(1):2–9. doi: 10.1093/carcin/bgr255.

Zhang Z, Garzotto M, Davis EW, Mori M, Stoller WA, Farris PE, Wong CP, Beaver LM, Thomas GV, Williams DE, et al. 2020. Sulforaphane bioavailability and chemopreventive activity in men presenting for biopsy of the prostate gland: a randomized controlled trial. Nutr Cancer. 72(1):74–87. doi: 10.1080/01635581.2019.1619783.

Zhong J, Yan W, Wang C, Liu W, Lin X, Zou Z, Sun W, Chen Y. 2022. BRAF inhibitor resistance in melanoma: mechanisms and alternative therapeutic strategies. Curr Treat Options Oncol. 23(11):1503–1521. doi: 10.1007/s11864-022-01006-7.